Title
Organization of microscale objects using a microfabricated optical fiber.

Journal
Optics letters, 33(18)

ISSN
0146-9592

Authors
Mohanty, SK
Mohanty, KS
Berns, MW

Publication Date
2008-09-01

DOI
10.1364/ol.33.002155

Published in final edited form as:
Opt Lett. 2008 September 15; 33(18): 2155–2157.

Organization of microscale objects using a microfabricated optical fiber

S. K. Mohanty[*], **K. S. Mohanty**, and **M. W. Berns**
Beckman Laser Institute, University of California-Irvine, Irvine, California 92612, USA

Abstract

We demonstrate the use of a single fiber-optic axicon device for organization of microscopic objects using longitudinal optical binding. Further, by manipulating the shape of the fiber tip, part of the emanating light was made to undergo total internal reflection in the conical tip region, enabling near-field trapping. Near-field trapping resulted in trapping and self-organization of long chains of particles along azimuthal directions (in contrast to the axial direction, observed in the case of large tip cone angle far-field trapping).

Optical manipulation of microscopic objects using spatially sculptured optical landscapes [1] coupled with optical binding [2] is gaining considerable interest for engineering self-assembled colloidal and biological structures. While far-field binding between microscopic objects has been demonstrated using elliptical beams [2,3] or two counterpropagating beams [4], near-field trapping and binding over a large area has been reported [5] at the interface of total internal reflection (TIR) occurring in a prism. Except for twofiber trapping [4], all other approaches have depth limitation. The two-fiber configuration requires critical alignment of the two counterpropagating beams and therefore restricts three-dimensional (3D) manipulation of the optically bound structure. Theoretical evaluation of the trapping force exerted by the microfocused beam from an axicon-tipped single fiber [6] and its use for in-depth trapping of cells [7] and low-index particles [8] has been demonstrated recently. An axicon (having a conical surface) can be used to turn a Gaussian beam into a Bessel beam, with greatly reduced diffraction and smallest optical confinement zones [9,10]. The micro-axicon fiber can trap at a larger distance from the fiber tip compared to a tapered fiber [11]. Here, we report optical binding of microscopic particles trapped in a single fiber-optic beam.

For fabrication of the axicon tip with varying tip cone angle, a two-step chemical etching using hydrofluoric acid was employed [7]. Figure 1 illustrates how Bessel-like beams having different propagation characteristics can be generated by engineering the axicon microstructure on the fiber. Starting with the fundamental mode of the fiber, $E_{fund} \approx \exp[-(X^2+Y^2)/\omega^2]$, where ω is the mode-field size, the electric field propagating from the tip can be described [12] as

[*]Corresponding author: smohanty@uci.edu.

$$E(x_0,y_0)\frac{\exp(ikz)}{i\lambda z}\exp\left[i\frac{k}{2z}(x_0^2+y_0^2)\right]\int_{-\infty}^{\infty}\int_{-\infty}^{\infty}\left\{E(x_1,y_1)\exp\left[i\frac{k}{2z}({x_1}^2+{y_1}^2)\right]\right\}\exp\left[-i\frac{2\pi}{\lambda z}(x_0x_1+y_0y_1)\right]\mathrm{d}x_1\mathrm{d}y_1, \quad (1)$$

where $E(x_1,y_1)$ is the field at the base of the micro-axicon, which can be calculated using E_{fund}, and accounting for the phase acquired along the axicon-tip region. *XY*-intensity distribution of the 800 nm beam transmitted through the axicon tip, calculated at two *Z* distances from the tip (fiber core size, 8 μm; refractive index of axicon, 1.5; cone angle, ~30°), is shown in Figs. 1(a) and 1(b). Figures 1(c) and 1(d) show typical beam profiles measured at distances of 5 and 15 μm from the tip. The measured beam profiles showed Bessel-like beam profiles with few concentric rings. The scattering force in the axial direction is minimized by the Bessel-like beam as compared to the beam from a lensed/tapered fiber. Owing to this special property of the Bessel–Gauss beam (having a small high-intensity region along the *Z* direction), a relatively less diverging beam can achieve single-beam optical tweezers as compared to Gaussian beam optical tweezers. In addition to an increase in propagation distance with a decrease in cone angle (data not shown), transmittance of the beam through the fiber tip decreased substantially, which was attributed to an increase in TIR at the tip [10].

The experimental setup consists of a TEM_{00} mode output of a cw Ti:sapphire laser beam (800 nm, Coherent Inc., USA) coupled to the microfabricated single-mode fiber. A 20 × microscope objective (MO) was used for imaging. Two 1 μm polystyrene particles suspended in phosphate-buffered saline (PBS) were trapped and raised to a height of a few mm from the coverslip. Figure 2(a) shows optical binding between two particles (in the encircled region) at a distance of ~3 μm from the tip. Analysis of images using cross-correlation techniques [13] provided positions of particles with nanometer resolution. The contrast was increased by region-of-interest selection and thresholding. The bottom right inset in Fig. 2(a) show a 3D intensity map of the two optically bound particles. The two optically bound particles remained almost at a fixed separation over the 10 min observation period. However, in the bound state, they were found to move in the axial direction within 3 to 6 μm. Translation of the fiber in three dimensions led to transportation of the (encircled) optically bound particles (data not shown). The distance between the two particles decreased as they moved away from the tip. Tracking of particles (1 and 2) as the fiber tip (dark line) was translated is shown as an inset [Fig. 2(b)]. Figure 2(b) shows the histogram of the separation between the optically bound particles measured over 30 s.

Figure 3(a) illustrates how far-field single fiber trapping and optical binding of a chain of microscopic particles could be achieved. For a cone angle of 60°, a truncated Bessel beam (power, 146 mW) trapping of polystyrene particles (diameter, 1 μm) was observed at a distance of ~5 μm from the tip. For a fixed cone angle (e.g., 90°), trapping stiffness along the axial direction measured by the equipartition theorem method [7] was found to depend on the size of the particle (2.0 pN/μm for 1 μm polystyrene versus 3.2 pN/μm for 2 μm polystyrene, for 60 mW trapping power). Similarly, trapping stiffness was found to depend on cone angle, e.g., 1.2 pN/μm for 60° cone angle and 2.0 pN/μm observed for a 90° cone angle tip, for a 1 μm particle trapped at a trapping power of 60 mW. This is due to the longer (~5 μm) propagation distance of the Bessel beam generated by the 60° tip. This ensured

transverse trapping of more particles along the axial direction. Figure 3(b) shows arrangement of a chain of ~20 particles along the beam propagation direction. This can be attributed to longitudinal optical binding [4] where each trapped particle acts as a lens to trap a subsequent particle near its focal point [Fig. 3(a)]. The difference between the Bessel–Gauss beam generated by the axicon-tip fiber and the conventional Bessel beam is the propagation distance. A conventional Bessel beam (focused through a MO) has a large propagation distance and therefore low axial-trapping stiffness, leading to two-dimensional (2D) optical trapping [14].

The optically bound chain could be displaced by translation of the fiber. Over a 15 min period, more particles aligned along the axial direction [Fig. 3(c)]. During the transverse motion of the long chain (achieved by movement of the fiber), when an obstacle [particles adhered to the glass substrate, marked by arrow in Fig. 3(d)] was encountered, the loose end of the optically bound chain oscillated around the obstacle [Figs. 3(d)–3(g)]. Though use of a larger cone angle (90°) led to more axially stable 3D Bessel beam trapping, the optically bound chain was shorter compared to the smaller cone angle (60°) tip.

In order to achieve near-field trapping, the cone angle was made small enough (≤30°) that a high percentage of the beam underwent TIR at the tip– water interface [Fig. 3(h)]. Since the strength of an evanescent wave decays rapidly with the distance from the place where it is generated, trapping volume is significantly reduced. The incidence critical angle for TIR is calculated to be ~63° (refractive index of the tip/water, 1.5/1.33) using Snell's law, which corresponds to a tip cone angle of 54°. Assuming all the rays to be parallel, none of the laser beam should exit a 30° cone angle tip. However, imperfection in the tip and the fact that not all rays inside the single-mode fiber travel in straight lines leads to leakage of the beam. In our case, stable far-field trapping in the axial direction was rarely observed [Figs. 3(i)–3(k)] since a small amount of laser power came out in the axial direction. Additionally, the propagation distance became longer (~8 μm), adding to the instability.

However, near-field trapping [5] at the interface between the tip and the water led to better trapping and thus self-organization of long stable chains of particles along the azimuthal directions. Owing to the exponentially decaying evanescent field [5,15] at the site of TIR, the closest trapped particle was found nearer to the surface of the tip in contrast to a few micrometers in the far-field case [Figs. 3(a)–3(g)]. Azimuthal binding of trapped particles may be affected by whispering gallery mode excitation in the beads. The azimuthal angles, at which the optically bound chains are formed, were found to vary from 30° to 75° [Fig. 3(c)]. Some of the near-field induced optically bound chains (1 and 4) lengthened [Figs. 3(i)–3(k)] over a period of time and became highly stable, while others at smaller azimuthal angles (2 and 3) shortened. Switching off the laser beam led to disorganization [Fig. 3(l)] of the particles. Metallization of the tip to enhance the evanescent field by the surface plasmon effect resulted in heating effects leading to convection and bubble formation (data not shown).

In conclusion, by shaping the axicon tip cone angle, single fiber optical trapping and binding in the farfield as well as near-field was achieved, leading to organization of microscopic particles. Since the trapping force on metallic particles in the Rayleigh regime is higher as

compared to dielectric particles, the axicon fiber can also be used to organize metallic nanoparticles and to study optical binding [16]. The proposed noninvasive axicon-tipped fiber can be used in multifunctional mode for in-depth trapping as well as for excitation of fluorophores and detection of backreflected light/fluorescence.

References

1. Grier DG. Nature. 2003; 424:810. [PubMed: 12917694]
2. Burns MM, Fournier JM, Golovchenko JA. Phys Rev Lett. 1989; 63:1233. [PubMed: 10040510]
3. Mohanty SK, Andrews JT, Gupta PK. Opt Express. 2004; 12:2746. [PubMed: 19475117]
4. Tatarkova SA, Carruthers AE, Dholakia K. Phys Rev Lett. 2002; 89:283901. [PubMed: 12513147]
5. Mellor CD, Bain CD. ChemPhysChem. 2006; 7:329. [PubMed: 16380953]
6. Mohanty SK, Mohanty KS. Proc SPIE. 2007; 6441:644116.
7. Mohanty SK, Mohanty KS, Berns MW. J Biomed Opt. 2008; 13:046805JBO.
8. Mohanty KS, Liberale C, Mohanty SK, Degiorgio V. Appl Phys Lett. 2008; 92:151113.
9. Grosjean T, Baida F, Courjon D. Appl Opt. 2007; 46:1994. [PubMed: 17384713]
10. Eah S, Jhe W. Rev Sci Instrum. 2003; 74:4969.
11. Liu Z, Guo C, Yang J, Yuan L. Opt Express. 2006; 14:12510. [PubMed: 19529686]
12. Goodman, JW. Introduction to Fourier Optics. McGraw-Hill; 1968.
13. Gelles J, Schnapp BJ, Sheetz MP. Nature. 1988; 331:450. [PubMed: 3123999]
14. Garcés-Chávez V, McGloin D, Melville H, Sibbett W, Dholakia K. Nature. 2002; 419:145. [PubMed: 12226659]
15. Gu M, Haumonte J, Micheau Y, Chon JWM, Gan X. Appl Phys Lett. 2004; 84:4236.
16. Zelenina AS, Quidant R, Nieto-Vesperinas M. Opt Lett. 2007; 32:1156. [PubMed: 17410267]

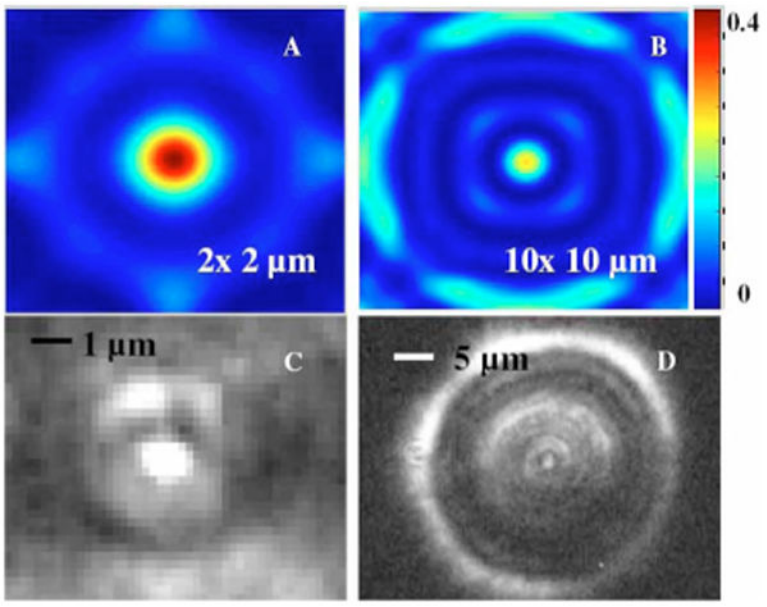

Fig. 1.

(Color online) (a), (b) *XY*-intensity distribution of the 800 nm beam transmitted through the fiber calculated at distances of 5 and 15 μm from the tip (fiber core size of 8 μm, refractive index of axicon as 1.5, cone angle of ~30°, and water as the medium). (c), (d) Measured beam profiles at distances of 5 and 15 μm.

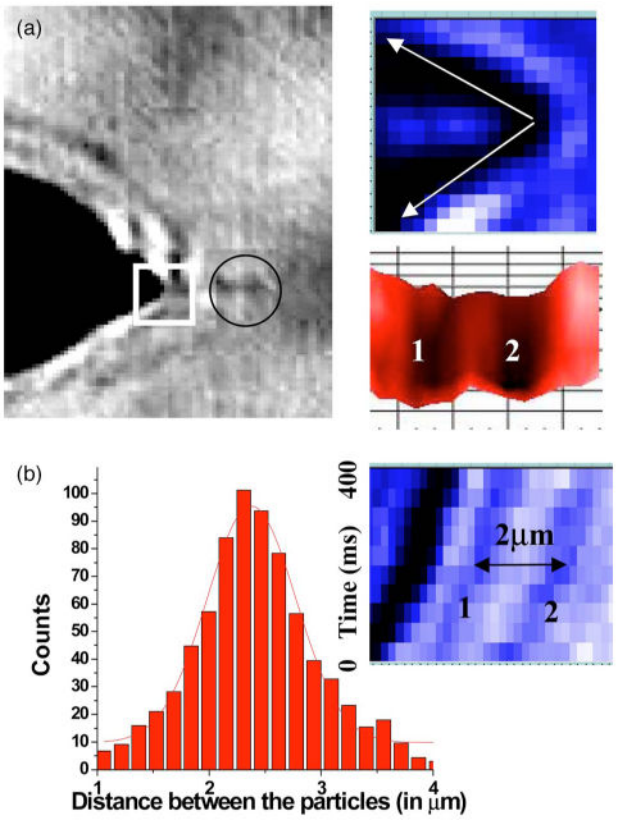

Fig. 2.

(Color online) (a) Optical binding of two 1 μm polystyrene particles in the encircled region near the fiber tip. Top right inset shows magnified rectangular area of the tip. Inset in the bottom right shows a 3D intensity map of the two optically bound particles. (b) Measured histogram of the distance between centers of two 1 μm optically bound particles. Inset shows tracking of the two particles (1 and 2) as the fiber tip (dark line) is translated.

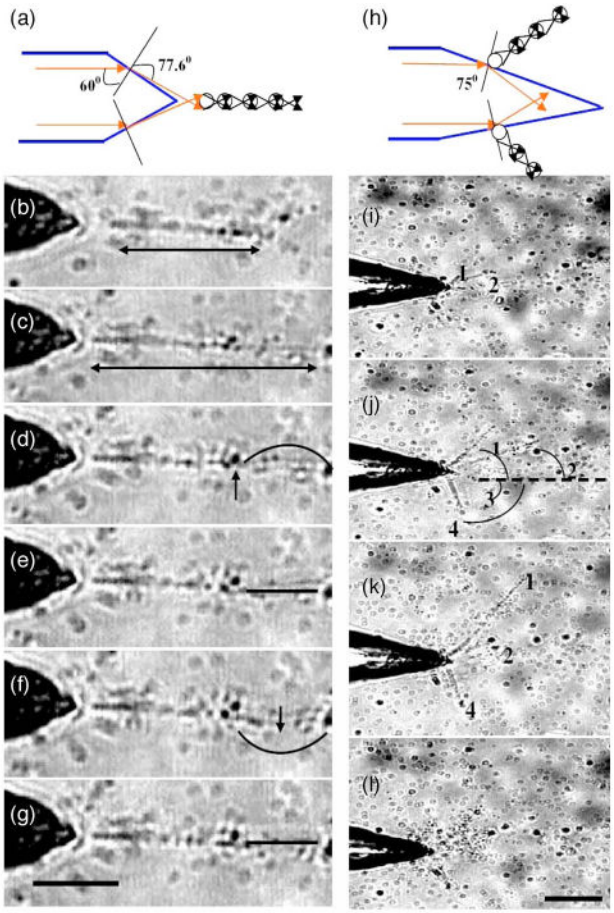

Fig. 3.

(Color online) (a) Ray optics schematic of longitudinal optical binding using large cone angle (e.g., 60°) tip. Optical trapping and binding leading to a chain of 1 μm polystyrene particles at 146 mW beam power (b). (c) Accumulation of particles in a long chain (~50 μm) after 15 min. (d)–(g) Oscillation (arrows show direction of movement) of part of the optically bound chain at the loose end. Images in (b)–(g) are the same magnification; scale bar, 10 μm. (h) Schematic of the near-field trapping and binding using small cone angle (e.g., 30°) tip. Digitized images of near-field trapped polystyrene particles at 68 mW beam power, after 1 min (i), 5 min (j), and 15 min (k). (l) Dispersion of the chain after the laser is turned off. Images in (i)– (l) are the same magnification; scale bar, 20 μm.